Radar Cross Section of General Three-Dimensional Scatterers

ALLEN TAFLOVE, MEMBER, IEEE, AND KORADA UMASHANKAR, SENIOR MEMBER, IEEE

Abstract—**Two disparate approaches—the finite-difference time-domain (FD-TD) method and the method-of-moments (MOM) surface-patch technique—which permit highly realistic modeling of electromagnetic scattering problems are compared. New results of induced surface currents and radar cross section are presented for an important three-dimensional canonical cube scatterer. It is shown that a high level of agreement for the two modeling approaches is obtained for this scattering example.**

Key Words—**Radar cross section, scatterers, three-dimensional, cube, finite-difference time-domain, method of moments.**

Index Code—**J10d.**

I. INTRODUCTION

GENERAL ELECTROMAGNETIC scattering problems have been difficult to treat with either analytical or numerical methods because of the complicating effects of curvatures, corners, apertures, and dielectric loading of structures. In an attempt to gain insight into scattering mechanisms using analytical and numerical approaches, it has been necessary to use canonical structures, rather than realistic models. Two potential alternate approaches which may permit more realistic modeling of scattering problems are the finite difference time-domain (FD-TD) method [1]-[12] and the method-of-moments (MOM) surface-patch technique [13]-[19]. These two modeling approaches are similar only in that they both permit a detailed treatment of general three-dimensional scattering problems in the resonant range. In fact, they have a substantially different theoretical foundation and numerical realization, as summarized below.

FD-TD: This is a direct solution of Maxwell's *time dependent* curl equations for the electric and magnetic fields at a regular lattice of points covering a *volume* of space that contains a scatterer. A fully *explicit* numerical algorithm is used to simulate real-time wave propagation and scattering. Field boundary conditions at adjacent dissimilar media are automatically satisfied by the curl-equations analog. The radiation condition is *not inherent*, and must be formulated separately to properly work in the near field and in the time domain. Sinusoidal steady-state results can be obtained for a sinusoidal wave source in the limit as the number of time steps is made sufficiently large. The latter approach can be viewed as being an *iterative solution* to the time-harmonic Maxwell equations.

MOM surface patching: This steps up a scheme for solving the *time-harmonic* integro-differential equation describing electric and magnetic field boundary conditions at the *surface* of a scatterer. An *implicit* numerical approach (matrix inversion) is used to solve the resulting set of simultaneous equations for the fields at the scatterer surface. The radiation condition is *implicit* in the formulation. Sinusoidal steady-state results are available immediately upon matrix inversion. This can be viewed as a *one-step solution* to the time-harmonic Maxwell equations.

The goal of this paper is to present the first detailed comparison of near- and far-field results for an important three-dimensional canonical scattering problem obtained using both the latest FD-TD and MOM triangular surface-patch modeling approaches [10], [12], [18], [19]. By comparing the computed results for scatterer surface currents and radar cross-section, it is shown that a high level of agreement of the two disparate modeling approaches is obtained for this scattering example.

Given the fundamental differences in basis and method of FD-TD and MOM, it can be argued that this agreement enhances confidence in each technique. Indeed, it can be argued that MOM must agree well with FD-TD (in the problem size range where each is applicable) if both techniques are valid models of the wave-scattering physics that occur in nature. To this end, an initial attempt has been made to investigate modeling of distinct near-field phenomena such as current singularity behavior at edges. Ideally, MOM and FD-TD would agree on edge behavior using no *a priori* assumptions regarding current singularity behavior. Here, however, it was found that MOM required incorporation of just such an *a priori* assumption to correspond with direct FD-TD results. (Use of a similar edge condition for FD-TD would probably relax its spatial resolution requirements.) Considerable work remains to examine how near- and far-field physics for both MOM and FD-TD is dependent upon such assumptions and the basic question of spatial resolution.

This paper will first briefly review the basis of the latest FD-TD and MOM triangular surface-patch approaches for modeling scattering problems. Results of these two methods for surface currents (magnitude and phase) and for far-scattered fields are then compared for the case of a metal cube illuminated by a plane wave at normal incidence to one face. The paper concludes with a discussion of the direction that research in the MOM and FD-TD modeling approaches may follow in the near future.

II. BASIS OF THE FD-TD METHOD FOR SCATTERING PROBLEMS

The FD-TD method is a direct solution of Maxwell's time-dependent curl equations. Recent research efforts have con-

Manuscript received January 14, 1983; revised August 11, 1983.

The authors are with the IIT Research Institute, 10 West 35th Street, Chicago, IL 60616.(312) 567-4490.

0018-9375/83/1100-0433$01.00

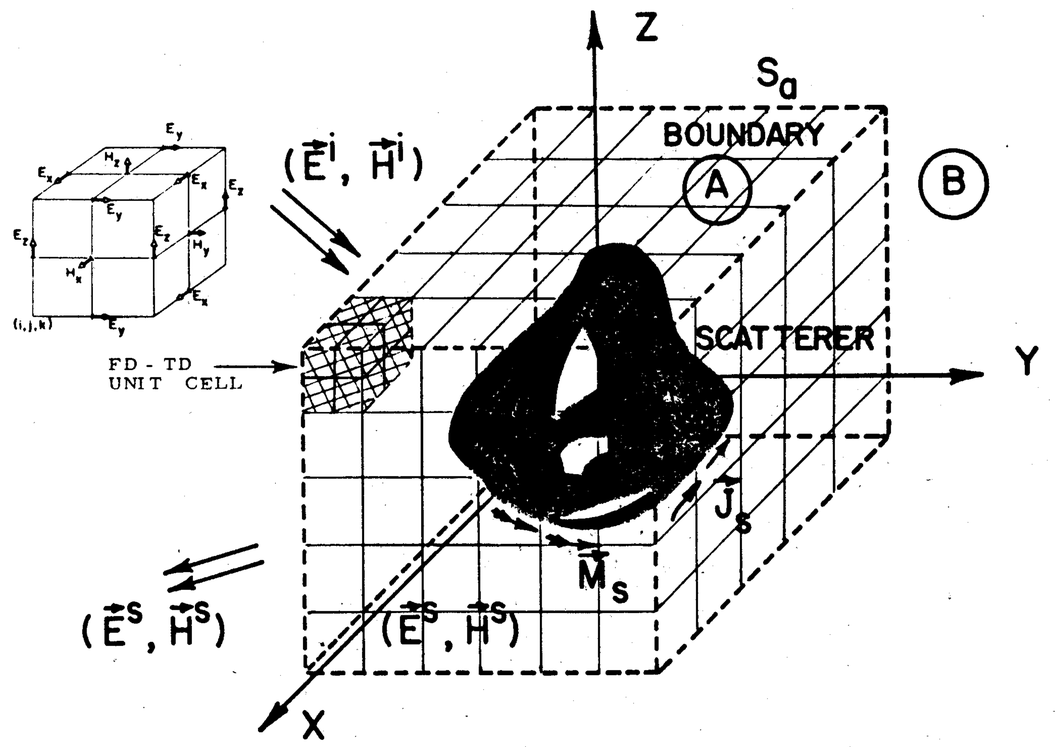

Fig. 1. Geometry of a general scatterer in free-space medium and FD-TD lattice arrangement.

centrated on examining the usefulness of applying the FD-TD method to model three-dimensional penetration and scattering problems, particularly involving structures having "volumetric complexity." This refers principally to structures having cavity-backed apertures that may be filled with complex media. Examples of such structures include missile seeker sections, which may have apertures for infrared or radar detectors leading to irregular interior cavities containing various metal and dielectric structures and electronic circuitry [11].

The goal of the FD-TD approach is to model the propagation of an electromagnetic wave into a volume of space containing a dielectric or conducting structure. By time-stepping, i.e., repeatedly implementing a finite-difference analog of the curl equations at each cell of the corresponding space lattice, the incident wave is tracked as it first propagates to the structure and then interacts with it via surface-current excitation, diffusion, penetration, and diffraction. Wave-tracking is completed when the desired late-time or sinusoidal steady-state behavior is observed at each lattice cell. The rationale for this procedure is that it achieves simplification by analyzing the interaction of the wave front with portions of the structure surface at a given instant in time, rather than attempting simultaneous solution of the entire problem. The following is a brief listing of key points on which the FD-TD method for scattering problems is based [1], [7]-[10], [12].

A. Time-Stepping Relations

Time-stepping for the FD-TD method is accomplished by an explicit finite-difference procedure due to Yee [1]. For a Cartesian cubic-cell space lattice, this procedure involves positioning the components of $\vec{E}$ and $\vec{H}$ about a unit cell of the lattice, as shown in Fig. 1, and evaluating $\vec{E}$ and $\vec{H}$ at alternate half-time steps. In this manner, centered difference expressions can be used for both the space and time derivatives to attain second-order accuracy in the space and time increments without requiring simultaneous equations to compute the fields at the latest time step. For example, the x component of the $\nabla \times \vec{E}$ equation [4], written as

$$\frac{\partial H_x}{\partial t} = \frac{1}{\mu}\left(\frac{\partial E_y}{\partial z} - \frac{\partial E_z}{\partial y}\right) \tag{1a}$$

is implemented as the following time-stepping relation for H_x:

$$H_x^{n+1/2}(i, j+1/2, k+1/2) = H_x^{n-1/2}(i, j+1/2, k+1/2) + \frac{\delta t}{\mu(i, j+1/2, k+1/2)\delta} \cdot \left[\begin{array}{l} E_y^n(i, j+1/2, k+1) - E_y^n(i, j+1/2, k) + \\ E_z^n(i, j, k+1/2) - E_z^n(i, j+1, k+1/2) \end{array}\right]. \tag{1b}$$

In (1b), it is assumed that all media are isotropic and time invariant; and that the space-time functional notation $F^n(i, j, k) = F(i\delta, j\delta, k\delta, n\delta t)$ applies, where $\delta = \delta x = \delta y = \delta z$ is the space increment, δt is the time increment, and i, j, k, and n are integers.

B. Implications for Computer Resource Requirements

The Yee system is termed fully explicit, since the new value of a field vector component at any lattice point depends only on existing field values stored in memory. The explicit formulation is particularly suited for parallel-processing or vector-array-processing computers. Also, the required memory and execution time increases only linearly with N, the total number of field components.

With the Yee formulation of the FD-TD algorithm, the value of N is clearly a function of the normalized electrical volume of a scatterer, e.g., $N \sim L^3$, where L = (scatterer characteristic dimension)/λ_0. For the MOM surface-patching approach, N is a function of only the normalized electrical surface area of a scatterer (if the scatterer has little or no internal complexity), e.g., $N \sim L^2$. For such scatterers, the aggregate computer resources needed to store and invert the MOM-derived impedance matrix vary with a dimensionality as low as $N^2 \sim L^4$ [20], which is little more than the FD-TD requirements. However, if the scatterer has "volumetric complexity", as defined earlier, the MOM requirements for N will tend towards L^3, rather than L^2. For such scatterers, the aggregate computer resources for the MOM approach will tend toward $N^2 \sim L^6$, significantly greater than the FD-TD dependence of L^3. As a result, it is possible that the FD-TD approach will find its most advantageous application to model structures with significant volumetric complexity, if modeling accuracy can be demonstrated for such structures.

It can be shown that the number of time steps required for the FD-TD technique is relatively *independent* of the electrical size of the scatterer being modeled, over a wide size range. Small scatterers have features which are usually tightly coupled (electrically), so that relatively many time steps are needed to permit wave energy to diffract from one feature to another, and back again, and back again, and so forth, to reach the sinusoidal steady state. Large scatterers have features which are usually more loosely coupled (electrically), reducing the need to extend time-stepping to model the physics of multiple-diffraction effects. The result is that a 25-wavelength scatterer may require no more than twice

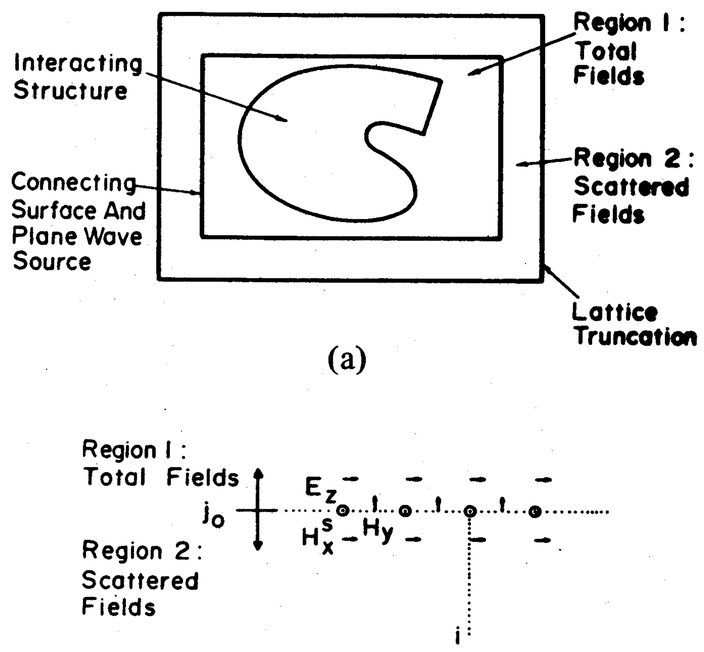

Fig. 2. Division of FD-TD lattice into total-field and scattered-field regions. (a) Lattice division. (b) Typical connecting conditions between regions.

the number of time steps of a 5-wavelength scatterer, if the space increment is held constant for both cases. In a more typical case where the space increment is reduced to define better geometrically the 5-wavelength scatterer, the number of time steps for the two cases may be nearly equal.

C. Total-Field/Scattered-Field Lattice Division

As shown in Fig. 2, the most recent FD-TD approaches [7]-[10], [12] divide the computation space into two regions separated by a rectangular surface. Region 1, denoted as the total-field zone, contains the scatterer. Region 2 surrounds Region 1 and is denoted as the scattered-field zone. The outer lattice planes bounding Region 2, called the lattice truncation planes, serve to implement the free-space radiation condition.

In Region 1, the scatterer of interest is mapped into the space lattice simply by assigning values of permittivity, conductivity, and permeability to each component of $\vec{E}$ and $\vec{H}$. In this manner, inhomogeneities or fine details of the scatterer can be modeled with a maximum resolution of one unit cell. Thin surfaces are modeled as stepped-edge sheets. Since total fields are computed in this region, no special handling of electromagnetic boundary conditions at media interfaces is needed because the curl equations generate these conditions in a natural way. Thus the basic computer program need not be modified to change from one scatterer to another. Further, the total-field formalism yields a very high computational dynamic range useful for modeling fields within cavities or in shadow regions.

The rectangle faces comprising the boundary between Regions 1 and 2 contain E- and H-field components which according to the Yee system of equations, require the formulation of various field-component differences across the boundary planes for the proceeding one time step. By either adding or subtracting appropriate values of the incident wave, a consistency relation can be enforced wherein total-field quantities are always subtracted from similar total-field quantities; and scattered-field quantities are always subtracted from scattered-field quantities. This enforcement of consistency serves to precisely connect the two regions, as well as generate

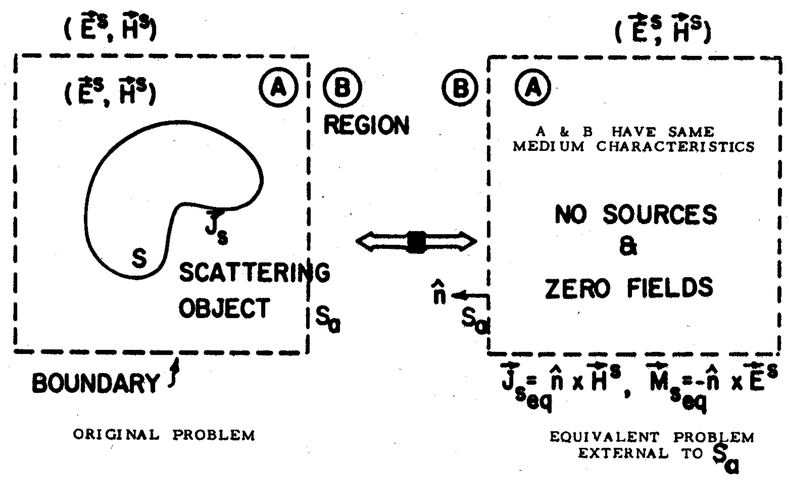

Fig. 3. Electromagnetic equivalence to transform near-fields to far-fields.

the desired incident wave of arbitrary angle of arrival and polarization [8]-[10], [12]. An alternative approach for incident-wave generation based on the Huygen's source formulation is discussed in [7].

The rectangle faces comprising the outer boundary of Region 2 are used to simulate the extension of the lattice to infinity. Recent work discussed in [9], [10], [12], [21], [22] has demonstrated such a radiation condition which is sufficiently accurate to permit only fractional-decibel perturbations of the fields in Regions 1 and 2 for most conditions.

D. Derivation of Sinusoidal Steady-State Data

Sinusoidal steady-state (phasor) data can be obtained from the FD-TD method either by:

a) directly programming a single-frequency incident plane wave, or
b) performing a separate Fourier transformation step on the pulse waveform response.

Both methods require time-stepping to a maximum time equal to several wave periods at the desired frequency. The second method has two additional requirements. First, a short-rise-time pulse suffers from accumulating waveform error due to overshoot and ringing as it propagates through the Yee space lattice. This leads to a numerical noise component which must be filtered before Fourier transformation. Second, Fourier transformation of many lattice-cell field-versus-time waveforms would significantly add to the total requirements for computer storage and execution time.

Recent work [10], [12] has shown that very accurate magnitude and phase information for sinusoidal steady-state FD-TD problems can be obtained by method a) above and observing the peak positive- and negative-going excursions of the fields over a complete cycle of the incident wave (after having time-stepped through 2-5 cycles of the transient period following the beginning of time-stepping). In this manner, the uncertainty introduced by possible decaying dc offsets of the field-versus-time waveform or by ambiguous phase reference points can be avoided.

E. Derivation of Far-Field Scattering Data

Far-field scattering data can be obtained with the FD-TD method by applying a powerful and flexible near-field to far-field transformation [8], [10], [12]. By reference to Fig. 3, a rectangular virtual surface S_a, which fully encloses the

scatterer, is located in the scattered-field region (Region 2 of Fig. 2). The tangential components of the scattered fields $\vec{E}^s$ and $\vec{H}^s$ are first obtained at S_a using FD-TD. Then, as indicated in Fig. 3(b), an equivalent problem is set up which is completely valid for Region B, external to S_a. The new excitation data are $\vec{J}_{s_{eq}}$ and $\vec{M}_{s_{eq}}$, the equivalent surface electric and magnetic currents, respectively, on S_a which are obtained according to [23]

$$\vec{J}_{s_{eq}}(\vec{r}) = \hat{n} \times \vec{H}^s(\vec{r}) \tag{2a}$$

$$\vec{M}_{s_{eq}}(\vec{r}) = -\hat{n} \times \vec{E}^s(\vec{r}) \tag{2b}$$

where $\hat{n}$ is the outward unit normal vector at the surface S_a.

The scattered far fields are given by the transform of the equivalent currents of (2a) and (2b) over the free-space Green's function [24], [25]. If (μ_0, ϵ_0) are the region-B medium characteristics with $k_0 = 2\pi/\lambda_0$ and $\eta_0 = 120\ \pi$, for θ and ϕ polarizations the following scattered far-field expressions are obtained:

$$E_\theta = (-jk_0\eta_0)\left[A_\theta + \frac{F_\phi}{\eta_0}\right] \tag{3a}$$

$$E_\phi = (-jk_0\eta_0)\left[A_\phi - \frac{F_\theta}{\eta_0}\right] \tag{3b}$$

where

$$A_\theta = A_x \cos\theta \cos\phi + A_y \cos\theta \sin\phi - A_z \sin\theta \tag{4a}$$

$$F_\theta = F_x \cos\theta \cos\phi + F_y \cos\theta \sin\phi - F_z \sin\theta \tag{4b}$$

$$A_\phi = -A_x \sin\phi + A_y \cos\phi \tag{4c}$$

$$F_\phi = -F_x \sin\phi + F_y \cos\phi \tag{4d}$$

and the potentials in the far-field region are given by

$$\begin{bmatrix}\vec{A},\\ \vec{F}\end{bmatrix} = \left(\frac{e^{-jk_0r}}{4\pi r}\right)\iint_{S_a}\begin{bmatrix}\vec{J}_{s_{eq}},\\ \vec{M}_{s_{eq}}\end{bmatrix} e^{jk_0r'\cos\xi}\, ds_a' \tag{5a}$$

$$r'\cos\xi = (x'\cos\phi + y'\sin\phi)\sin\theta + z'\cos\theta. \tag{5b}$$

The radar cross section *RCS* is calculated as the ratio

$$RCS = 4\pi r^2\left[\frac{E_\theta{}^2 + E_\phi{}^2}{E_\theta{}^{i2} + E_\phi{}^{i2}}\right], \qquad r \to \infty. \tag{6}$$

where $E_\theta{}^i$ and $E_\phi{}^i$ are the corresponding components of the incident plane-wave excitation.

This approach to computing the far scattered fields is very promising since a) the near-field data for arbitrary scatterers can be obtained in a straightforward manner using the FD-TD method; and b) the transformation of the near-field data to the far field is computationally simple and independent of the nature of the scatterer which resides within the integration surface S_a. The complete bistatic radar cross section is a natural result of this procedure, for a given incident angle and polarization of the illuminating wave. For problems involving variable incidence and/or polarization of the illuminating wave, new FD-TD data are required for each selected incident-wave condition.

III. BASIS OF THE MOM SURFACE-PATCH MODEL

General arbitrary-shaped scattering bodies can be analyzed based on a frequency-domain integral-equation/boundary-value problem approach. A popular technique for the numerical solution which implements this approach is the method of moments [26]. This method is particularly suited for low-frequency scattering problems, but can be applied to bodies spanning approximately 1 wavelength in three dimensions [18], [19].

The following formulations of the method of moments have been found to be generally suited for certain scattering bodies based upon their geometry and material characteristics.

1) *Conducting Scatterers* (homogeneous, isotropic).
   a) Electric-field integral-equation formulation (EFIE) for closed and open bodies.
   b) Magnetic-field integral-equation formulation (MFIE) for closed bodies.
2) *Dielectric Scatterers* (homogeneous, isotropic).
   Combined-field integral-equation formulation (CFIE).

Recent work has concentrated on Case 1) [18], [19], especially in the development of the triangular-patch model for arbitrary scatterers. Research efforts are underway on Case 2) for dielectric scatterers.

To treat arbitrary-shaped conducting bodies [18], the EFIE formulation is generally used. On Fig. 4(a), if S denotes the surface of an open or closed body, the scattered electric field is given by

$$\vec{E}^s = -j\omega\vec{A} - \nabla\phi \tag{7}$$

where the magnetic vector potential and the scalar potential are defined as

$$\vec{A}(\vec{r}) = \frac{\mu_0}{4\pi}\iint_S \vec{J}(\vec{r}')G(\vec{r},\vec{r}')\, ds' \tag{8}$$

$$\phi(\vec{r}) = \frac{1}{4\pi\epsilon_0}\iint_S \rho^e(\vec{r}')G(\vec{r},\vec{r}')\, ds' \tag{9}$$

$$G(\vec{r},\vec{r}') = \frac{e^{-jk_0|\vec{r}-\vec{r}'|}}{|\vec{r}-\vec{r}'|} \tag{10}$$

and where (μ_0, ϵ_0) are scalar constants representing the permeability and permittivity of the surrounding medium; $\vec{J}$ and ρ^e are the unknown electric current and charge distributions induced on the conducting scatterer; and $R = |\vec{r} - \vec{r}'|$ is the distance between an arbitrarily located observation point $\vec{r}$ and a source point $\vec{r}'$ on S. Both $\vec{r}$ and $\vec{r}'$ are defined with respect to a global coordinate origin.

An integro-differential equation for $\vec{J}$ is derived [19] by enforcing the boundary condition $\hat{n} \times (\vec{E}^i + \vec{E}^s) = 0$ on S,

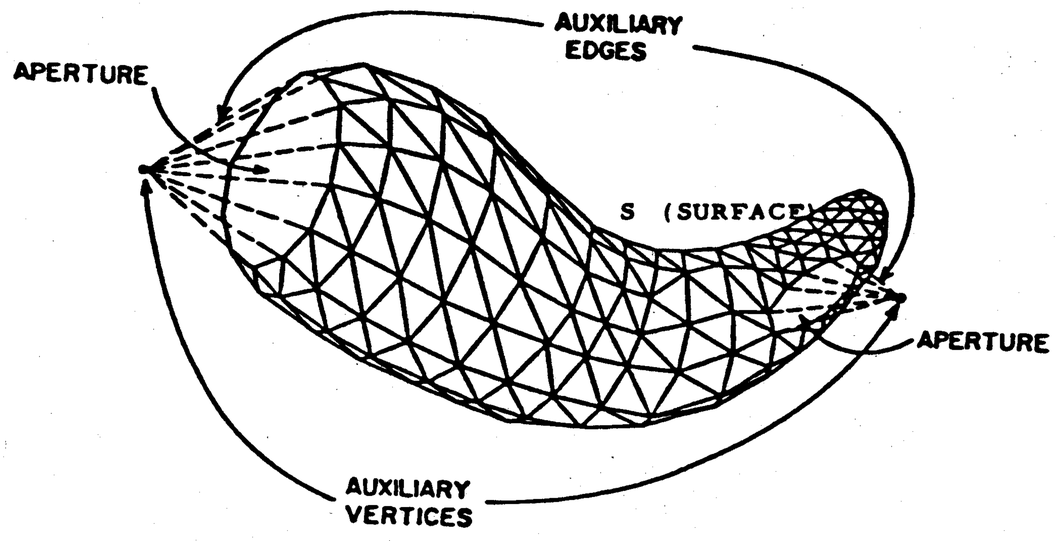

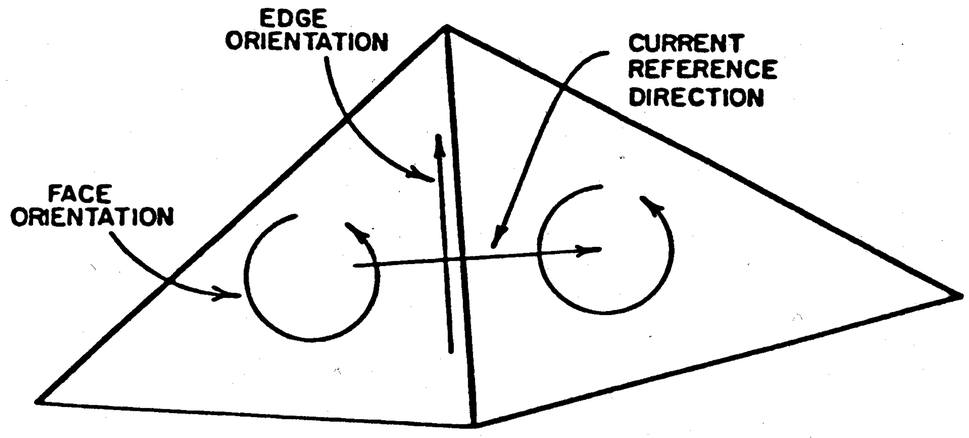

Fig. 4. Scatterer with triangular-patch modeling [18], [19].

obtaining

$$-\vec{E}_{\tan}{}^{i} = (-j\omega\vec{A} - \nabla\phi)_{\tan}, \qquad \vec{r} \text{ on } S. \tag{12}$$

In arbitrary surface modeling, the above EFIE has the advantage that it applies to both open and closed bodies, whereas the MFIE applies only to closed surfaces [18]. On the other hand, for arbitrarily shaped objects the EFIE is considerably more difficult to apply than the MFIE.

For modeling arbitrarily shaped surfaces, planar triangular-patch models (an example [18], [19] of which is shown in Fig. 4(a) and (b)) have been found to be particularly appropriate. Since triangular patches are capable of accurately conforming to any geometrical surface and boundary, the patch scheme is easily described to the computer, and a varying patch density can be used according to the resolution required in the surface geometry or current. This patching method permits the straightforward construction of MOM basis functions defined on the triangular patches which are free of line charges, Fig. 4(b).

In [18] and [19], planar triangular-patch modeling and the MOM [26] were applied to develop numerical procedures using the EFIE formulation to treat scattering by arbitrarily shaped conducting bodies. An efficient computer code based on this formulation was described which is capable of handling either open or closed and arbitrarily curved structures of finite extent. Discounting computer limitations, the code can, in principle, treat any conducting object whose surface is orientable, connected (or multiply-connected), and free of intersecting surfaces. *An updated version of this computer program* was used to obtain benchmark data for the surface currents and scattered fields for the conducting cube scatterer discussed next.

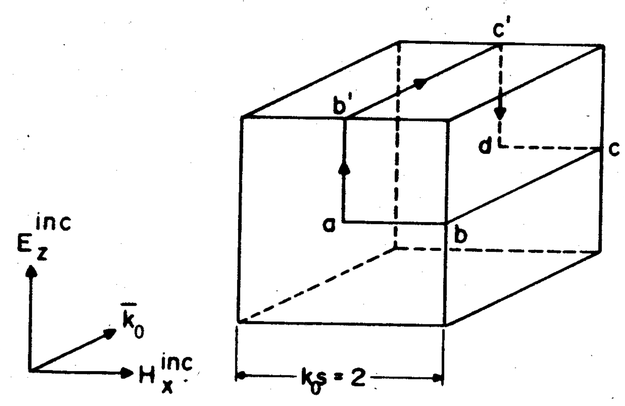

Fig. 5. Geometry of metal-cube scatterer.

IV. COMPARISON OF FD-TD AND MOM NUMERICAL RESULTS

This section presents comparative numerical results obtained using the most recent formulations of the FD-TD [10], [12] and MOM triangular surface-patch techniques [18], [19] for the surface currents and far scattered fields of a canonical three-dimensional scatterer, a conducting cube, illuminated by a plane wave. It is shown that a very high degree of correspondence exists between the results obtained by these two disparate approaches.

A. Scatterer Geometry

Fig. 5 illustrates the basic geometry of the cube scattering problem. The cube was assumed to have the electrical size $k_0 s = 2$, where s = side width of cube. The plane-wave excitation was assumed to have the field components $E_z{}^i$ and $H_x{}^i$ and propagate in the $+y$ direction (normal incidence to one side of the cube). For the FD-TD analysis, the cube was embedded in a 48 X 48 X 48-cell spatial lattice (663 552 unknown field components), and each side of the cube was spanned by 400 square cells (20 X 20 lattice-cell divisions). For the MOM analysis, each face of the cube was spanned by either 18 triangular patches or 32 triangular patches (to test the convergence of the patch model). The 18-patch/face MOM model required the filling and inversion of a 162 X 162 system matrix. The 32-patch/face MOM model required the filling and inversion of a 288 X 288 system matrix. These particular sizes for the FD-TD and MOM systems were selected because they have approximately equal computer costs (about \$200 to \$300). A more detailed discussion of computer resource requirements will follow after presentation of the modeling results.

B. Comparative Surface Currents

Figs. 6 and 7 graph the comparative results for the FD-TD and MOM/triangular-patch analysis of the magnitude and phase of the surface electric current along two straight-line loci traversing the cube surface, as shown in Fig. 5. Locus $\overline{abcd}$ is parallel to the incident magnetic field; currents plotted along this locus will show the effects of the edge singularities of the cube. Locus $\overline{ab'c'd}$ is parallel to the incident electric field; currents plotted along this locus are the "looping currents" driven by the wave electric field around the scatterer. The FD-TD computed surface current is taken as $\hat{n} \times \vec{H}_{\tan}$, where $\hat{n}$ is the unit normal vector at the cube surface, and $\vec{H}_{\tan}$ is the FD-TD value of the magnetic field parallel to the cube surface, but at a distance of 0.5 space cell from the surface. (The displacement of the H-component from the cube

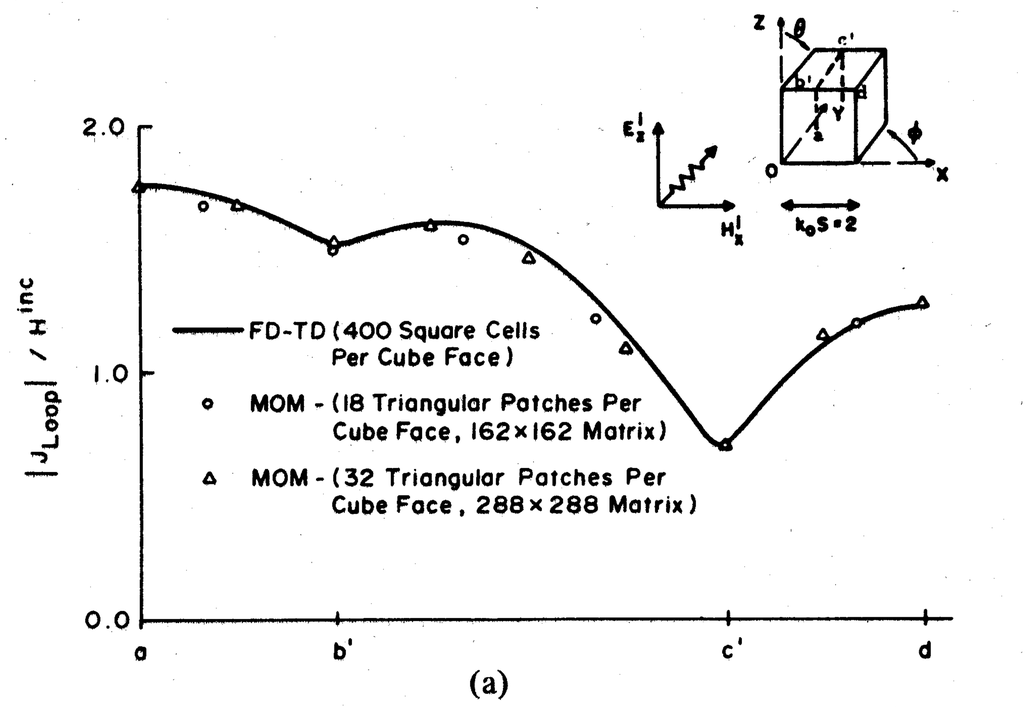

(a)

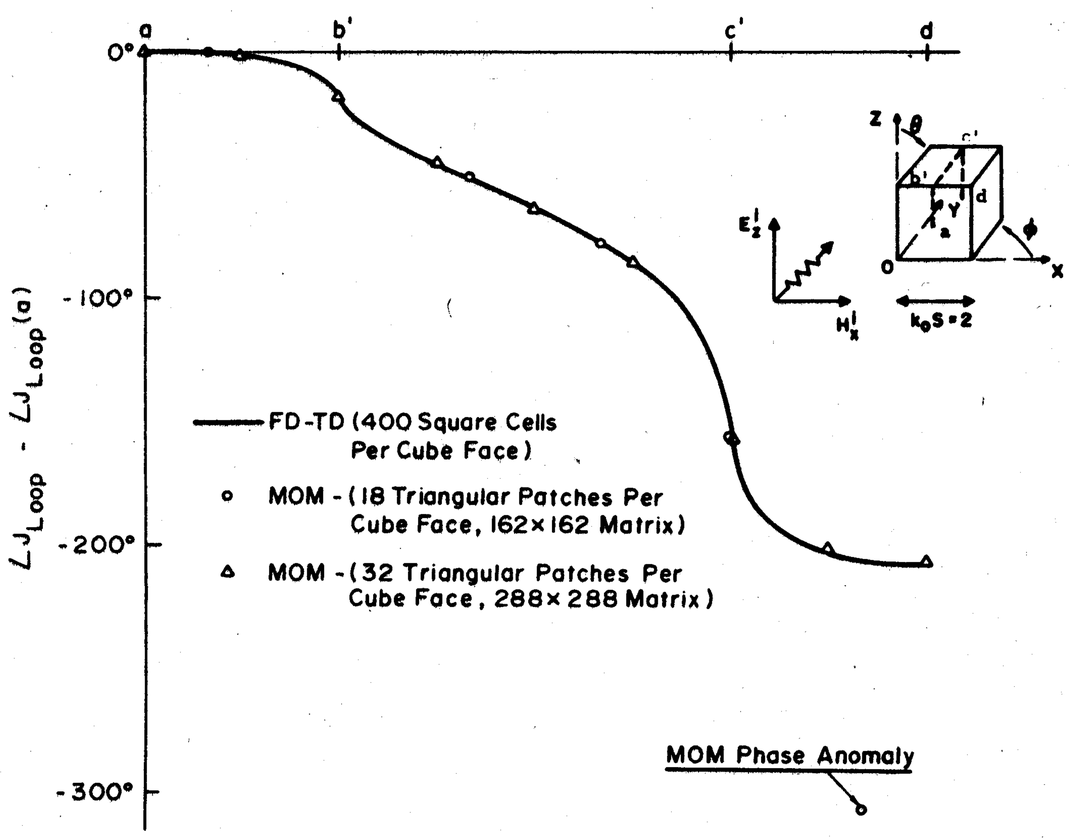

(b)

Fig. 6. (a) Magnitude of looping current, center vertical cut. (b) Phase of looping current, center vertical cut.

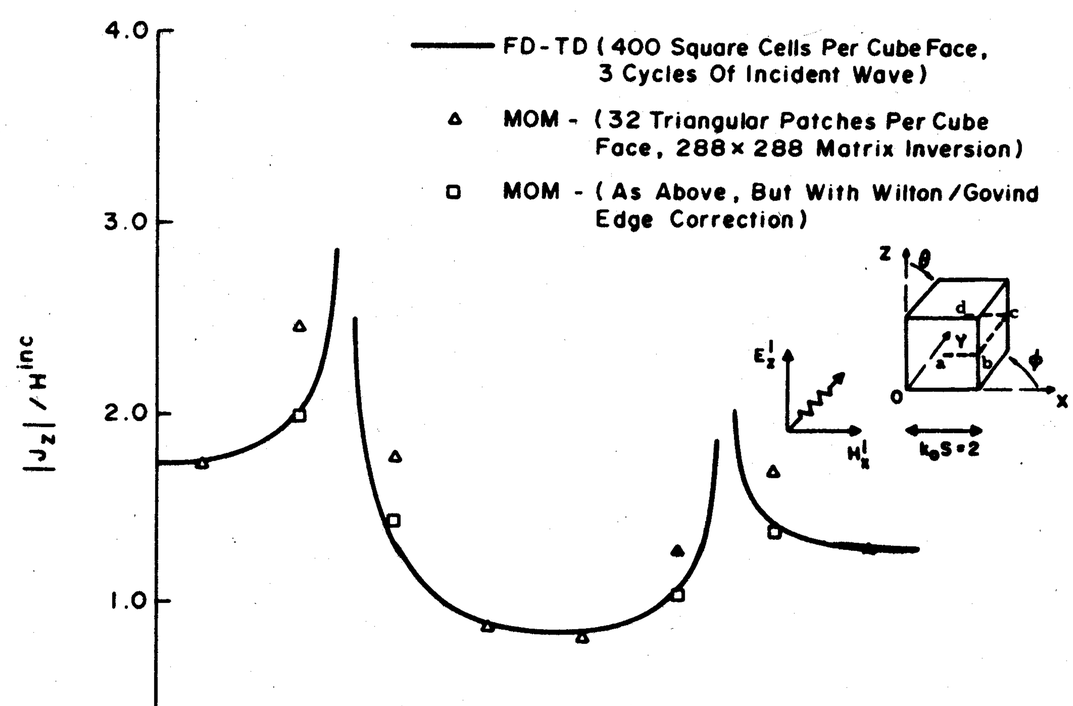

(a)

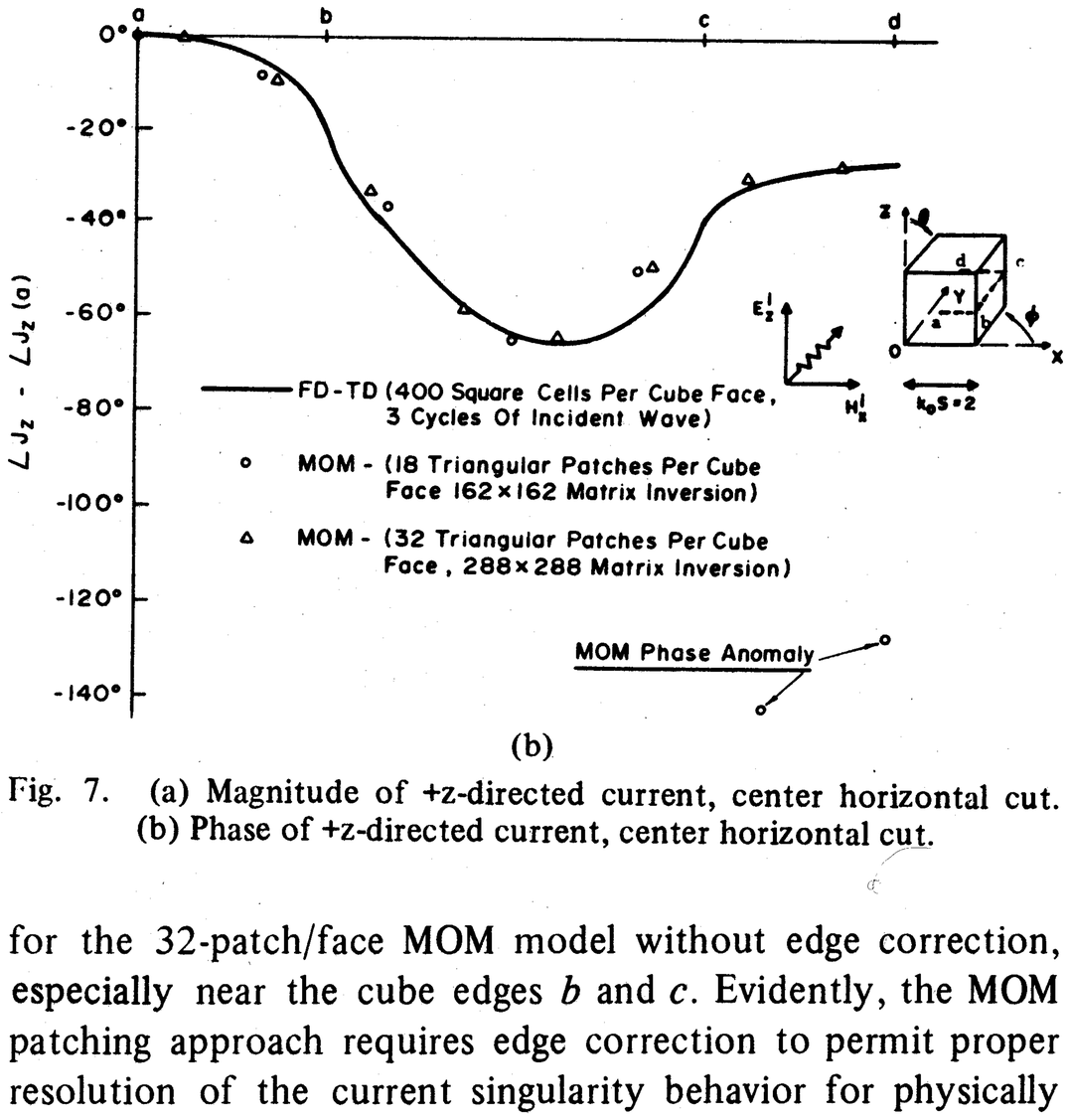

(b)

Fig. 7. (a) Magnitude of +z-directed current, center horizontal cut. (b) Phase of +z-directed current, center horizontal cut.

surface is a consequence of the spatially-interleaved nature of the *E*- and *H*-components of the FD-TD lattice).

In Fig. 6(a), the magnitude of the FD-TD computed looping current agrees with the 32-patch/face MOM solution to better than ±2.5 percent (±0.2 dB) at all comparison points along locus $\overline{ab'c'd}$. It should be noted that the 32-patch/face MOM model yields better magnitude agreement with the FD-TD results than the 18-patch/face MOM model.

In Fig. 6(b), the phase of the FD-TD computed looping current agrees with the 32-patch/face MOM solution to better than ±1° at all comparison points along locus $\overline{ab'c'd}$. It should be noted that the lower resolution 18-patch/face MOM model yields a phase anomaly of almost −100° in the shadow region. The MOM phase is corrected to coincide with the FD-TD results upon going to the higher resolution 32-patch/face MOM model. This type of slow convergence of phase has been noted in previous applications of the MOM surface-patch approach, in particular the case of the bent plate [27].

In Fig. 7(a), the FD-TD computed magnitudes agree with the edge-corrected [28] 32-patch/face MOM model to better than ±2.5 percent (±0.2 dB) at all comparison points along locus $\overline{abcd}$. Obvious slow convergence behavior is noted for the 32-patch/face MOM model without edge correction, especially near the cube edges *b* and *c*. Evidently, the MOM patching approach requires edge correction to permit proper resolution of the current singularity behavior for physically realizable numbers of patches.

In Fig. 7(b), the phase of the FD-TD computed *z*-directed current agrees with the 32-patch/face MOM model to better than ±10° along locus $\overline{abcd}$. The 18-patch/face MOM model is again seen to have substantial slow convergence in the shadow region. In fact, the switch from 18 patches/face to 32 patches is seen to result in better phase agreement with the FD-TD model at nonshadow points as well.

C. Comparative Scattered Far-Fields

Fig. 8 shows the bistatic radar cross-section (RCS) for the conducting-cube scatterer shown in Fig. 5. The RCS results are computed in two ways. First, the discrete plotted points are found by applying the near-to-far field relations of (2)-(6) to FD-TD-computed near-field data. Second, the continuous line is derived by directly integrating the induced surface electric currents on the cube that were computed using the MOM surface-patching technique. Good agreement (to

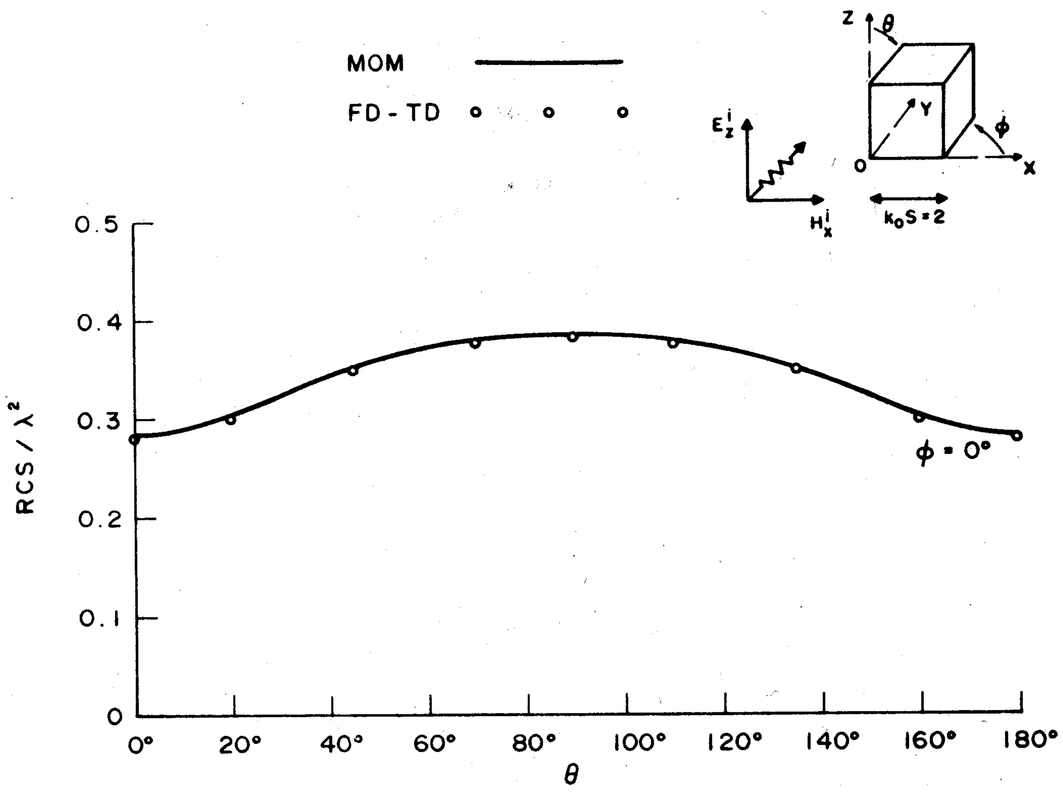

Fig. 8. Scattering cross section of the conducting cube scatterer.

better than ±1 percent or ±0.09 dB) between the two sets of RCS results is obtained.

D. Comparative Computer Resources

It is difficult to compare directly the computer resources for the particular FD-TD and MOM approaches tested, since a) neither computer program is presently optimized for minimum running time or storage; b) the programs were run on different computers (Cray-1S used for FD-TD, Cyber 203 used for MOM); and c) insufficent convergence-analysis runs were performed to test the agreement of the results as the FD-TD space increment is increased. Nevertheless, the following comments can be supported.

a) At least one-half of the total computation resources needed for the MOM surface-patching model were devoted to filling the impedance matrix.
b) Without changes in the means of solving the MOM system of equations, such as by using an acceptable iterative scheme, increasing the system matrix much beyond 288 × 288 may present problems in terms of computer storage and running time, as well as accuracy of the final result (the latter depending upon the degree of ill-conditioning of the matrix).
c) Even with a computationally accurate and efficient means of MOM matrix solution (such that only about N^2 operations are needed, where N is the number of field or current unknowns), scatterers having volumetric complexity as discussed in Section II-B may require aggregate computer resources approaching an L^6 dependence, where L is a normalized characteristic dimension of the scatterer.
d) Scatterers having volumetric complexity can be modeled using FD-TD with aggregate computer resources proportional only to L^3. However, the accuracy of such models remains to be demonstrated, especially for relatively coarse lattice-cell sizes approaching $0.1\lambda_0$, which would be necessary to implement FD-TD models of three-dimensional structures spanning 5 or more wavelengths. Demonstration of accuracy for such models would point the way to considerably larger models, taking advantage of the relatively slow (order of L^3) computer-resource dependence and the appearance of capable supercomputers.

V. POSSIBLE DIRECTIONS OF RESEARCH

Extension of the MOM surface-patching model to larger and more-realistic scatterers, including those with volumetric complexity, will likely require: a) incorporation of dielectric media into the model; b) resolution of remaining questions concerning convergence of the magnitude and phase of the computed currents and fields; c) examination of three-dimensional structures with empty and loaded cavities; and 4) investigation of iterative (and other innovative) approaches to solving the large matrices produced by the MOM technique.

Extension of the FD-TD model to larger and more realistic scatterers will likely require: a) demonstration of accuracy for coarse lattice sizes approaching $0.1\lambda_0$; b) demonstration of accuracy for structures having curved surfaces, cavities, and volumetric complexity; c) examination of the effect of scatterer "Q" or ringing time upon the number of time steps needed to attain the sinusoidal steady state; and d) incorporation of graded lattices, field equivalences, or hybrid approaches to permit treatment of very large structures that have only a limited number of complex substructures that chiefly impact scattering.

Extension of both the MOM surface-patching and FD-TD approaches will require incorporation of the latest features and capabilities of computers, array-processing computers, and multiprocessor computers. Available central memories and floating-point operation rates of these machines will largely determine the maximum size and complexity of problems that can be modeled, if the problems listed above can be solved.

VI. CONCLUSIONS

General electromagnetic scattering problems are difficult to treat. In this paper, two disparate approaches—FD-TD and MOM—which permit analysis and modeling of realistic scattering problems, are summarized and compared. New results based on these two methods for induced surface currents and radar cross section are compared for the three-dimensional canonical case of a conducting metal cube illuminated by a plane wave.

This paper has shown for the first time (for three-dimensional problems) that FD-TD and MOM can provide excellent agreement of computed surface currents and far fields for a canonical scatterer. Because the level of agreement is very high, confidence in each approach is increased. This paper consequently asserts that FD-TD is a viable approach for scattering problems that is at least competitive with MOM or other comparable approaches.

ACKNOWLEDGMENT

The authors would like to thank Dr. S. M. Rao of Rochester Institute of Technology, Rochester, NY, for assistance during the development of this program.

REFERENCES

[1] K. S. Yee, "Numerical solution of initial boundary value problems involving Maxwell's equations in isotropic media," *IEEE Trans. Antennas Propagat.*, vol. AP-14, pp. 302–307, May 1966.

[2] C. D. Taylor, D. H. Lam, and T. H. Shumpert, "Electromagnetic pulse scattering in time-varying inhomogeneous media," *IEEE Trans. Antennas Propagat.*, vol. AP-17, pp. 585–589, Sept. 1969.

[3] D. E. Merewether, "Transient currents induced on a metallic body of revolution by an electromagnetic pulse," *IEEE Trans. Electromagn. Compat.*, vol. EMC-13, pp. 41–44, May 1971.

[4] A. Taflove and M. E. Brodwin, "Numerical solution of steady-state electromagnetic scattering problems using the time-dependent Maxwell's equations," *IEEE Trans. Microwave Theory Tech.*, vol. MTT-23, pp. 623–630, Aug. 1975.

[5] R. Holland, "Threde: A free-field EMP coupling and scattering code," *IEEE Trans. Nucl. Sci.*, vol. NS-24, pp. 2416–2421, Dec. 1977.

[6] K. S. Kunz and K. M. Lee, "A three-dimensional finite-difference solution of the external response of an aircraft to a complex transient EM environment: Part I—The method of its implementation," *IEEE Trans. Electromagn. Compat.*, vol. EMC-20, pp. 328–333, May 1978.

[7] D. E. Merewether, R. Fisher, and F. W. Smith, "On implementing a numeric Huygen's source scheme in a finite-difference program to illuminate scattering bodies," *IEEE Trans. Nucl. Sci.*, vol. NS-27, pp. 1819–1833, Dec. 1980.

[8] A. Taflove and K. R. Umashankar, "A hybrid FD-TD approach to electromagnetic wave backscattering," in *1981 URSI/APS—Int. Symp. Proc.*, (Los Angeles, CA), June 1981, p. 82.

[9] G. Mur, "Absorbing boundary conditions for the finite-difference approximation of the time-domain electromagnetic-field equations," *IEEE Trans. Electromag. Compat.*, vol. EMC-23, pp. 377–382, Nov. 1981.

[10] A. Taflove and K. R. Umashankar, "User's code for FD-TD," IIT Research Institute, Chicago, IL, Final Rep. to Rome Air Development Center, Griffiss AFB, NY, no. RADC-TR-82-16, Contract F30602-80-C-0302, Feb. 1982.

[11] A. Taflove and K. R. Umashankar, "A hybrid moment method/finite difference time domain approach to electromagnetic coupling and aperture penetration into complex geometries," *IEEE Trans. Antennas Propagat.*, vol. AP-30, pp. 617–627, July 1982.

[12] K. R. Umashankar and A. Taflove, "A novel method to analyze electromagnetic scattering of complex objects," *IEEE Trans. Electromagn. Compat.*, vol. EMC-24, pp. 397–405, Nov. 1982.

[13] N. C. Albertsen, J. E. Hansen, and N. E. Jenson, "Computation of radiation from wire antennas on conducting bodies," *IEEE Trans. Antennas Propagat.*, vol. AP-22, pp. 200–206, Mar. 1974.

[14] L. L. Tsai, D. G. Dudley, and D. R. Wilton, "Electromagnetic scattering by a three-dimensional conducting rectangular box," *J. Appl. Phys.*, vol. 45, Oct. 1974, pp. 4393–4400.

[15] A. Sankar and T. C. Tong, "Current computation on complex structures by finite element method," *Electron. Lett.*, vol. 11, pp. 481–482, Oct. 1975.

[16] E. H. Newman and D. M. Pozar, "Electromagnetic modeling of composite wire and surface geometries," *IEEE Trans. Antennas Prop.*, vol. AP-26, pp. 784–789, Nov. 1978.

[17] J. Singh and A. T. Adams, "A non-rectangular patch model for scattering from surfaces," *IEEE Trans. Antennas Propagat.*, vol. AP-27, pp. 531–535, July 1979.

[18] D. R. Wilton, S. M. Rao, and A. W. Glisson, "Electromagnetic scattering by surfaces of arbitrary shape," in *Applications of the Method of Moments to Electromagnetic Fields*, B. J. Strait, Ed. Orlando, FL: SCEEE Press, 1980, pp. 139–170.

[19] S. M. Rao, D. R. Wilton, and A. W. Glisson, "Electromagnetic scattering by surfaces of arbitrary shape," *IEEE Trans. Antennas Propagat.*, vol. AP-30, pp. 409–418, May 1982.

[20] E. K. Miller and A. J. Poggio, "Moment-method techniques in electromagnetics from an application viewpoint," in *Electromagnetic Scattering*, P. L. E. Uslenghi, Ed. New York: Academic, 1978, ch. 9.

[21] B. Engquist and A. Majda, "Absorbing boundary conditions for the numerical simulation of waves," *Math. Comput.*, vol. 31, pp. 629–651, July 1977.

[22] G. A. Kriegsmann and C. S. Morawetz, "Solving the Helmholtz equation for exterior problems with variable index of refraction: I," *SIAM J. Sci. Stat. Comput.*, vol. 1, pp. 371–385, Sept. 1980.

[23] S. A. Schelkunoff, "Field equivalence theorems," *Commun. Pure Appl. Math.*, vol. 4, pp. 43–59, June 1951.

[24] J. Van Bladel, *Electromagnetic Fields*. New York: McGraw Hill, 1964.

[25] R. F. Harrington, *Time Harmonic Electromagnetic Fields*. New York: McGraw Hill, 1961, ch. 3.

[26] R. F. Harrington, *Field Computation by Moment Methods*. New York: MacMillan, 1968.

[27] S. M. Rao, Department of Electrical Engineering, Rochester Institute of Technology, Rochester, NY, private communication to K. Umashankar.

[28] D. R. Wilton and S. Govind, "Incorporation of edge conditions in moment method solutions," *IEEE Trans. Antennas Propagat.*, vol. AP-25, pp. 845–850, Nov. 1977.